

Article

Calibration of Finn Model and UBCSAND Model for Simplified Liquefaction Analysis Procedures

Jui-Ching Chou ¹ , Hsueh-Tusng Yang ² and Der-Guey Lin ^{3,*}

¹ Department of Civil Engineering, National Chung Hsing University, Taichung 40227, Taiwan; jccchou@nchu.edu.tw

² Public Works Department, Pingtung County Government, Pingtung City 900219, Taiwan; x0988430023@gmail.com

³ Department of Soil and Water Conservation, National Chung Hsing University, Taichung 40227, Taiwan

* Correspondence: dglin@dragon.nchu.edu.tw

Abstract: Soil-liquefaction-related hazards can damage structures or lead to an extensive loss of life and property. Therefore, the stability and safety of structures against soil liquefaction are essential for evaluation in earthquake design. In practice, the simplified liquefaction analysis procedure associated with numerical simulation analysis is the most used approach for evaluating the behavior of structures or the effectiveness of mitigation plans. First, the occurrence of soil liquefaction is evaluated using the simplified procedure. If soil liquefaction occurs, the resulting structural damage or the following mitigation plan is evaluated using the numerical simulation analysis. Rational and comparable evaluation results between the simplified liquefaction analysis procedure and the numerical simulation analysis are achieved by ensuring that the liquefaction constitutive model used in the numerical simulation has a consistent liquefaction resistance with the simplified liquefaction analysis procedure. In this study, two frequently used liquefaction constitutive models (Finn model and UBCSAND model) were calibrated by fitting the liquefaction triggering curves of most used simplified liquefaction analysis procedures (NCEER, HBF, JRA96, and T-Y procedures) in Taiwan via FLAC program. In addition, the responses of two calibrated models were compared and discussed to provide guidelines for selecting an appropriate liquefaction constitutive model in future projects.



Citation: Chou, J.-C.; Yang, H.-T.; Lin, D.-G. Calibration of Finn Model and UBCSAND Model for Simplified Liquefaction Analysis Procedures. *Appl. Sci.* **2021**, *11*, 5283.

<https://doi.org/10.3390/app11115283>

Academic Editor: Stuart Hardy

Received: 12 April 2021

Accepted: 26 May 2021

Published: 7 June 2021

Publisher's Note: MDPI stays neutral with regard to jurisdictional claims in published maps and institutional affiliations.



Copyright: © 2021 by the authors. Licensee MDPI, Basel, Switzerland. This article is an open access article distributed under the terms and conditions of the Creative Commons Attribution (CC BY) license (<https://creativecommons.org/licenses/by/4.0/>).

1. Introduction

Soil-liquefaction-related hazards (lateral spreading, settlement of shallow foundations, uplift of underground structures, etc.) can severely damage structures or result in a considerable loss of life and property. Therefore, it is important to evaluate the stability and safety of structures against soil liquefaction. In practice, the evaluation is usually performed in three steps: (1) a simplified liquefaction analysis procedure or a cyclic test is used to evaluate the occurrence of soil liquefaction at a site during the design earthquake; (2) if the site is liquefied, effects of liquefaction hazards on structures are evaluated via an empirical procedure, a numerical simulation analysis, or a physical model test; and (3) a mitigation plan is necessary if structures are damaged due to liquefaction hazards. The effectiveness of a mitigation plan can also be evaluated via an empirical procedure, a numerical simulation analysis, or a physical model test. However, because of limited budgets and tight schedules, physical model tests are rarely used in practice. Instead, the simplified liquefaction analysis or the cyclic test used in the first step combined with the numerical simulation analysis used in the second and third steps become the most used approaches in practice.

In the numerical simulation analysis, an appropriate liquefaction constitutive model is required to model the soil liquefaction phenomenon. The liquefaction constitutive

model should have a consistent liquefaction resistance with the simplified liquefaction analysis procedure or experiment results used in the first step of the evaluation to obtain reasonable and comparable evaluation results in the second and third steps. Therefore, the input parameters of the liquefaction constitutive model should be calibrated to capture key aspects (liquefaction triggering and post-liquefaction deformation) of the simplified liquefaction analysis procedure or the cyclic test results [1].

In the past few decades, liquefaction constitutive models were improved from loose coupled effective stress models (e.g., Finn model) to fully coupled effective stress models (e.g., UBCSAND model and PM4SAND model). However, it remains a difficult task for engineers to choose an appropriate liquefaction constitutive model and representable values of model input parameters. Given that the techniques for sampling undisturbed sand samples (e.g., frozen sampling) are expensive and difficult, most projects do not obtain undisturbed sand samples; as such, reliable cyclic test results cannot be achieved. Therefore, the results of site-specific cyclic tests are usually not available; instead, the simplified liquefaction procedure is used to evaluate the occurrence of soil liquefaction on a site. When numerical analysis is needed for subsequent evaluations, many engineers assign the input parameters of the liquefaction constitutive model following the model's default values without performing a proper model calibration. This practice results in an inconsistent liquefaction resistance (cyclic resistance ratio, CRR) between the simplified liquefaction analysis procedure and the liquefaction constitutive model, leading to numerical simulation results that are not representable and comparable.

Among all liquefaction constitutive models, the Finn model and the UBCSAND model are widely used to explore liquefaction behaviors or liquefaction-related hazards in research or practical projects [2–9]. In these projects, the Finn model or the UBCSAND model were calibrated against dynamic test results [2,5,6,9], physical modeling test results [2,4,5,8], or data from real earthquake cases [4,7,9]. However, none of these projects were calibrated for simplified liquefaction procedures (NCEER, HBF, JRA96, and T-Y procedures) [10–13] commonly used in Taiwan. Therefore, when subsequent numerical simulation is needed, no calibrated input parameters can be used as references for engineers.

In this study, the Finn and UBCSAND models were calibrated by fitting the liquefaction triggering curves of NCEER, HBF, JRA96, and T-Y procedures [10–13] via FLAC program. In addition, model responses of the Finn model and the UBCSAND model were compared to explore model limitations. Results of this study provide engineers with a valuable reference for evaluating liquefaction hazards.

2. Constitutive Models

2.1. Finn Model

Martin et al. [14] noted that the irrecoverable volume strain (causing the fluid pressure change) and the cyclic shear strain amplitude of sand are related, and this relationship is independent of the confining stress. In addition, the accumulation rate of the volumetric strain decreases as the accumulated volumetric strain increases. An incremental shear volume coupling equation for sand under simple shear loading was proposed as follows:

$$d\varepsilon_v = C_1(\gamma - C_2\varepsilon_v) + (C_3\varepsilon_v^2 / (\gamma + C_4\varepsilon_v)), \quad (1)$$

where $d\varepsilon_v$ is the volumetric strain increment per cycle of shear strain, ε_v is the accumulated volumetric strain, γ is the amplitude of shear strain of the stress cycle in the calculation, and C_1 to C_4 are model constants related to the relative density of sand.

Byrne [15] proposed an alternative form of $d\varepsilon_v$ that has fewer model constants and is simpler than the original form [14]:

$$d\varepsilon_v / \gamma = C_1(\exp(-C_2\varepsilon_v / \gamma)), \quad (2)$$

where C_1 and C_2 are model constants related to the relative density of sand.

In Equation (2), C_1 controls the amount of the volumetric strain increment, and C_2 controls the rate of the volume strain accumulation. Byrne [15] provided relationships between model constants (C_1 and C_2) and the SPT N-value as a reference for users.

In FLAC [16], a built-in constitutive model, the Finn model, was coded and incorporated Equations (1) and (2) into the Mohr–Coulomb model to simulate the dynamic pore pressure generation under cyclic loading. In practice, Equation (2) [15] is mostly used because of its convenience and simplicity.

2.2. UBCSAND Model

The UBCSAND model [17,18] is a simple elastoplastic stress/strain model for simulating the liquefaction phenomenon of sand with a relative density less than 80%. The elastic and plastic responses of the model are briefly described in this section. The elastic response is assumed to be isotropic and governed by shear modulus, G^e , and bulk modulus, B^e , as follows:

$$G^e = K_G^e \times P_a \times (\sigma'/P_a)^{ne}, \quad (3)$$

$$B^e = K_B^e \times P_a \times (\sigma'/P_a)^{me}, \quad (4)$$

where K_G^e is the elastic shear modulus number which can be related to the SPT N-value, P_a is the atmospheric pressure, σ' is the mean effective stress in the plane of loading, ne is the exponent variable that relates the elastic shear modulus to the mean effective stress, K_B^e is the elastic bulk modulus number (which depends on Poisson's ratio), and me is the elastic exponent variable that relates the bulk modulus to the mean effective stress.

Plastic responses are divided into the plastic shear strain, γ^p , and the plastic volumetric strain, ε_v^p , controlled by the yield surface and the flow rule. The yield surface is represented by a radial line from the origin in $\sigma'-\tau$ space (mean effective stress–shear stress space, Figure 1). When the shear stress ratio ($\eta = \tau/\sigma'$) changes, the plastic shear strain increment, $d\gamma^p$, occurs as follows:

$$d\gamma^p = (\sigma'/G^p) \times d\eta, \quad (5)$$

$$G^p = G_i^p \times (1 - (\eta/\eta_f \times R_f))^2, \quad (6)$$

$$G_i^p = K_G^p \times P_a \times (\sigma'/P_a)^{np}, \quad (7)$$

where G^p is the plastic shear modulus, $d\eta$ is the stress ratio increment, G_i^p is the plastic shear modulus at a low shear stress ratio level, η_f ($= \sin \varphi_{peak}$) is the failure stress ratio, φ_{peak} is the peak friction angle, R_f is the failure ratio, K_G^p is the plastic shear modulus number, and np is an exponent variable that relates the plastic shear modulus to the mean effective stress.

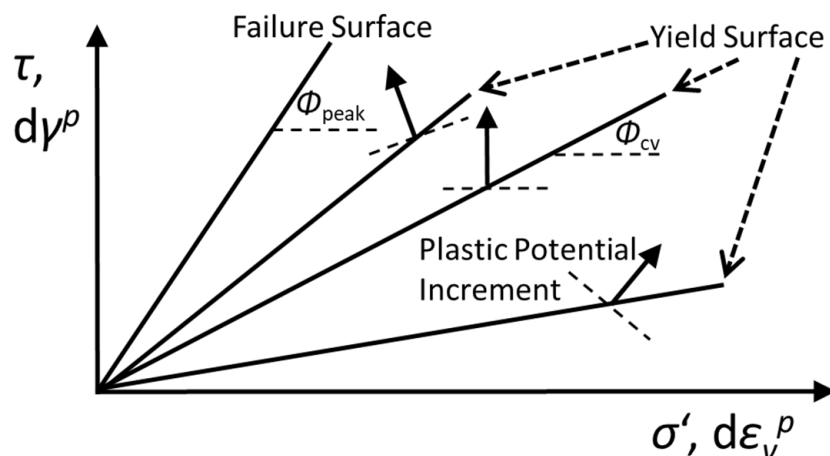


Figure 1. Yield surface, flow rule, and directions of plastic potential increments of the UBCSAND model.

A non-associated flow rule is adopted to connect the plastic volumetric strain increment, $d\varepsilon_v^p$, with the plastic shear strain increment, $d\gamma^p$, as follows:

$$d\varepsilon_v^p = (\sin \varphi_{cv} - \tau / \sigma') \times d\gamma^p, \quad (8)$$

where φ_{cv} is the constant volume friction angle or phase transformation angle. The direction of the plastic potential increment (i.e., the direction of the arrow on the yield surface) is shown in Figure 1. When the shear stress ratio η ($= \tau / \sigma'$) is equal to $\sin \varphi_{cv}$, there is zero plastic volumetric strain increment, and the material is in a constant-volume condition. When η is higher than $\sin \varphi_{cv}$, $d\varepsilon_v^p$ is negative, and the material is in a dilation condition. When η is lower than $\sin \varphi_{cv}$, $d\varepsilon_v^p$ is positive, and the material is in a contraction condition. The detailed information of the UBCSAND model is described in the literature [17–19].

The UBCSAND model was coded with FLAC [16] and validated by many studies [17,18,20–24] via application to centrifuge tests, laboratory tests, and earthquake measurements. Beaty and Byrne [19] provide a set of calibrated model input parameters against the liquefaction triggering curve of the NCEER procedure [10].

3. Methodology of Model Calibration

In this study, the constitutive models are calibrated using a single-element simulation of a cyclic undrained direct simple shear (DSS) test for four simplified liquefaction analysis procedures, including NCEER [10], HBF [11], JRA96 [12], and T-Y [13] procedures.

The initial stress condition is the K_0 (coefficient of earth pressure at rest) condition. The liquefaction criteria specify that the excess pore pressure ratio, r_u (= excess pore pressure/vertical effective consolidation stress), is equal to or greater than 95% at 15 cycles of uniform shear loading under one atmosphere (101 kPa) vertical effective consolidation stress (σ_{vc}'). Given that the laboratory test results for these simplified liquefaction analysis procedures were lacking, the Finn model and the UBCSAND model were calibrated by fitting the liquefaction triggering curves of these simplified procedures (Figure 2). For simplicity and comparison purposes, the constitutive models were both calibrated at selected SPT N-values ($(N_1)_{60cs} = 5, 10, 15, 20, 25, 30$). $(N_1)_{60cs}$ is the equivalent clean-sand SPT-N value at the energy ratio of 60% and under one atmosphere overburden stress.

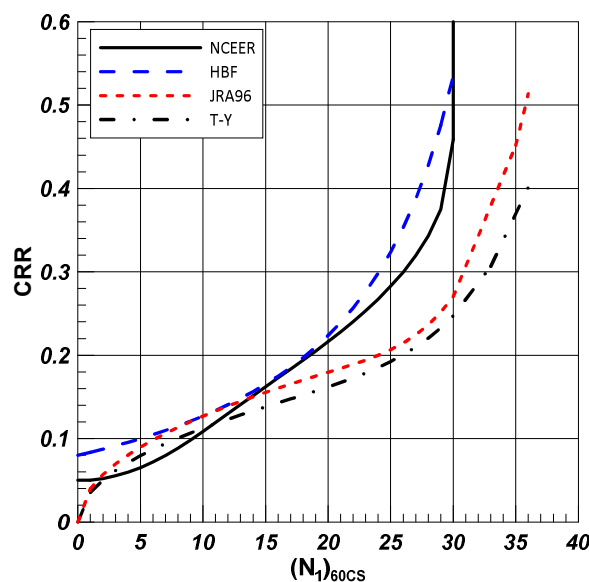


Figure 2. Liquefaction triggering curves of four simplified liquefaction analysis procedures.

The primary parameters of the Finn model with Byrne formulation are listed in Table 1. In this study, only C_2 was adjusted to fit the liquefaction triggering curves. C_1 and C_3 were values adopted from those proposed by Byrne [15], and other parameters were adopted

equations suggested by Beaty and Byrne [19]. Because the Finn model cannot fully simulate the shear modulus degradation under cyclic loadings, it was combined with FLAC's built-in hysteretic model during the calibration to achieve reasonable predictions of shear strain and volumetric strain.

Table 1. Input parameters of the Finn model with Byrne formulation in FLAC.

Parameter ¹	Meaning	Parameter ¹	Meaning
<i>friction</i>	friction angle, φ	<i>ff_c2</i> ²	C_2 of Equation (1)
<i>cohesion</i>	cohesion, C		
<i>dilation</i>	dilation angle, Ψ		
<i>shear</i>	shear modulus, G	<i>ff_c3</i> ²	C_3 , threshold shear strain—the shear strain below which volumetric strain will not be produced
<i>bulk</i>	bulk modulus, B		
<i>ff_c1</i> ²	C_1 of Equation (1)		

¹ Parameter title in the FLAC program. ² $C_1 = 8.7 \times ((N_1)_{60cs}) - 1.25$; $C_1 \times C_2 = 0.4$; $C_3 = 0.005\%$ [15].

The primary parameters of the UBCSAND model are listed in Table 2. The plastic shear modulus, G^p , is the key factor affecting the accumulation of the excess pore pressure and the CRR. The calibration process was simplified by adjusting the paraemeters related to plastic shear modulus (K_G^p and np) and maintaining other parameters same with the values provided by Beaty and Byrne [19]. The UBCSAND model can model the shear modulus degradation behavior, and no supplementary hysteretic model is needed.

Table 2. Input parameters of the UBCSAND model in FLAC.

Parameter ¹	Meaning	Parameter ¹	Meaning
<i>m_n160</i>	$(N_1)_{60cs}$	<i>m_rf</i>	failure ratio, R_f
<i>m_kge</i>	elastic shear modulus number, K_G^e	<i>m_hfac1</i> ²	accounts for the confining stress effect on the CRR
<i>m_ne</i>	elastic shear exponent, ne	<i>m_hfac2</i> ²	shear modulus factor to modify the rate of pore pressure generation
<i>m_kbe</i>	elastic bulk modulus number, K_B^e	<i>m_hfac3</i> ²	factor to modify post-liquefaction dilation response
<i>m_me</i>	elastic bulk exponent, me	<i>m_hfac4</i> ²	factor to control the plastic shear strains after liquefaction and soil dilation
<i>m_kgp</i>	plastic shear modulus number, K_G^p		
<i>m_np</i>	plastic shear exponent, np		
<i>m_phif</i>	peak friction angle, φ_{peak}		
<i>m_phicv</i>	constant-volume friction angle, φ_{cv}		

¹ Parameter title in the FLAC program. ² Model parameters of the UBCSAND model.

Relationships of the input parameters provided by Beaty and Byrne [19] are listed in Table 3 and described as follows. The small strain shear modulus (G_{max}) is estimated using equations in the literature [25,26]:

$$G_{max} = 21.7 \times (K_2)_{max} \times P_a \times (\sigma'/P_a)^{0.5}, \quad (9)$$

$$(K_2)_{max} = 3.5 \times (D_R)^{2/3} = 20 \times ((N_1)_{60cs})^{1/3}, \quad (10)$$

where $(K_2)_{max}$ is a modulus parameter, P_a is atmospheric pressure, σ' is the mean effective stress in the plane of loading, and D_R is the relative density of sand. Then, G_{max} and K_G^e can be expressed as follows:

$$G_{max} = 21.7 \times 20 \times ((N_1)_{60cs})^{1/3} \times P_a \times (\sigma'/P_a)^{0.5}, \quad (11)$$

$$K_G^e = 21.7 \times 20 \times ((N_1)_{60cs})^{1/3} \text{ and } ne = 0.5, \quad (12)$$

Table 3. Calibrated parameters of the UBCSAND model [19].

Parameter	Value or Relationship	Parameter	Value or Relationship
K_G^e	$21.7 \times 20 \times ((N_1)_{60cs})^{0.333}$	φ_{cv}	33°
K_B^e	$0.7K_G^e$	R_f	$1.1((N_1)_{60cs})^{-0.15} < 0.99$
K_G^p	$K_G^e \times ((N_1)_{60cs})^2 \times 0.003 + 100$	m_hfac1^1	$a \times (\sigma'/P_a)^b$
$ne/me/np$	$0.5/0.5/0.4$	m_hfac2	1
φ_{peak}	$\varphi_{cv} + 0.1(N_1)_{60cs} + \max(0, ((N_1)_{60cs} - 15)/5)$	m_hfac3	1
		m_hfac4	1

$$^1 a = 1.05 - 0.03(N_1)_{60cs} + 0.004((N_1)_{60cs})^2 - 0.000185((N_1)_{60cs})^3 + 2.92 \times 10^{-6}((N_1)_{60cs})^4; b = 1/(-0.424 - 0.259(N_1)_{60cs} + 0.00763((N_1)_{60cs})^2).$$

The constant-volume friction angle (φ_{cv}) was chosen as the typical value for quartz sands ($\varphi_{cv} = 33^\circ$). The other inputs (φ_{peak} , K_G^p , np , R_f , m_hfac1) in Table 3 were obtained based on the calibration process presented in Beaty and Byrne [19].

4. Results and Discussion

4.1. Finn Model

Tables 4 and 5 list the calibrated inputs for all four simplified liquefaction analysis procedures. The friction angle (φ) was φ_{peak} in Table 3 with a small modification, and the dilation angle, $\Psi (= \varphi - \varphi_{cv})$, is the difference between φ and φ_{cv} . Cohesion (C) was assigned a value of 1 kPa for numerical simulation stability. The model parameters C_1 and C_3 followed the suggested equations and values of Byrne [15]. The Finn model was combined with a FLAC built-in hysteretic model (the Hardin hysteretic model) [27] to model the shear modulus degradation curve of sand [25]. The shear modulus reduction equation of the Hardin hysteretic model is expressed as follows:

$$G/G_{max} = 1/(1 + (\gamma/\gamma_{ref})), \quad (13)$$

Table 4. Calibrated parameters of the Finn model–Byrne formulation in FLAC.

Parameter	Value or Relationship	Parameter	Value or Relationship
φ	$\varphi_{cv} + 0.1(N_1)_{60cs}$	C_1	$8.7((N_1)_{60cs})^{-1.25}$
C	1 kPa	C_2	$C_1 \times C_2 = C_Finn$
T_{cut}	0	C_3	0.005%
Ψ	$(\varphi - \varphi_{cv})$	φ_{cv}	33°
$G (= G_{max})$	Equation (11)	hysteretic model	
B	$1.33G$		$\gamma_{ref} = 0.06\%$

Table 5. Calibrated C_Finn .

$(N_1)_{60cs}$	NCEER	HBF	JRA96	T-Y
5	0.35	0.90	0.80	0.56
10	0.35	0.50	0.34	0.34
15	0.35	0.43	0.29	0.19
20	0.35	0.40	0.21	0.13
25	N.A.	N.A.	0.11	0.10

N.A. = no answer.

where G is the current shear modulus under the cyclic loading, G_{max} is the small strain shear modulus (i.e., G in Table 4), γ is the current shear strain under the cyclic loading, and γ_{ref} is the reference shear strain corresponding to γ when the shear modulus reduction ratio is 0.5 ($=G/G_{max}$).

Table 5 shows that for NCEER and HBF procedures, the values of C_Finn at $(N_1)_{60cs} = 25$ could not be determined because the excess pore pressure ratio, r_u , was not able to meet

the liquefaction criteria. Values of C_{Finn} ($= C_1 \times C_2$) for $(N_1)_{60cs}$ between the values listed in Table 5 could be linearly interpolated.

4.2. UBCSAND Model

In the UBCSAND model calibration, the parameters related to the plastic shear (K_G^p) and np) were adjusted, and all other input parameters were kept the same as the values and equations listed in Table 3. After several trials, in which an np of 0.4 was maintained and K_G^p was changed to fit the liquefaction triggering curves (Table 6), the model responses yielded the best results. Because the case of $(N_1)_{60cs} = 30$ in NCEER and HBF procedures were not able to meet the liquefaction criteria, the relationships of NCEER and HBF procedures were only valid to $(N_1)_{60cs} = 25$.

Table 6. Calibrated K_G^p of the UBCSAND model.

Procedure	$(N_1)_{60cs}$ Range	Relationship ¹
NCEER	5~25	$K_G^p = 0.06X^3 + 5.65X^2 + 18.18X + 160$
HBF	5~25	$K_G^p = 0.79X^3 - 8.71X^2 + 66.85X + 350$
JRA96	5~30	$K_G^p = -0.26X^3 + 9.02X^2 + 6.74X + 280$
T-Y	5~30	$K_G^p = -0.16X^3 + 6.29X^2 + 8.00X + 210$

¹ $X = ((N_1)_{60cs} - 5)$.

4.3. Comparisons of Undrained Cyclic DSS Responses

Beatty and Perlea [28] compared the responses of the Finn model and the UBCSAND model from dynamic analyses of an embankment. However, the element responses between the Finn model and the UBCSAND model were not discussed. In this section, the element responses of undrained cyclic DSS simulations of the Finn model and the UBCSAND model are compared and discussed in terms of (1) stress–strain relationships (shear stress–shear strain, shear stress–vertical effective stress, and excess pore pressure accumulation); and (2) factors affecting the CRR (the number of uniform loading cycles, overburden stress, and static shear stress).

Figure 3 shows the relationships between shear stress–shear strain and shear stress–vertical effective stress. The responses of JRA96 $(N_1)_{60cs} = 10$ cases were selected as an illustration. Both models treat the unloading response as elastic to simplify the formulation of the model. The accumulation of the volumetric strain (i.e., the accumulation of excess pore pressure ratio, r_u , or the decrease in the vertical effective stress) of the Finn model occurs every half cycle of loading, whereas the UBCSAND model accumulates during each cycle of loading. The key features that a liquefaction constitutive model attempts to simulate are: (1) banana loop—the plastic shear modulus reduces and increases during a shear stress reversal (from positive shear stress to negative shear stress and vice versa) when the soil reaches the initial liquefaction; and (2) butterfly loop—a significant drop in the vertical effective stress and a subsequent increase in the vertical effective stress when the soil reaches the initial liquefaction.

The stress–strain curve and the stress path in Figure 3b show that the UBCSAND model could imitate the banana loop and the butterfly loop well because the model tracks the stress ratio history to account for the loading reversal effect on the plastic shear modulus. In addition, the UBCSAND model captured the accumulation of the shear strain during cyclic loading better than the Finn model.

Curves of excess pore water pressure generation are shown in Figures 4 and 5 against curves suggested by Seed et al. [29]. The cycle ratio is defined as the number of cycles (N) divided by the number of cycles to liquefaction (N_{liq}). When the cycle ratio was close to 1.0 (or 0.8~1.0), the excess pore pressure ratio, r_u , of high $(N_1)_{60cs}$ cases ($= 20, 25, 30$) of the UBCSAND model was relatively low (Figure 5) because of the high dilation angle of these cases. Nevertheless, in general, both models were able to capture the general trend of the accumulated excess pore pressure during cyclic loading.

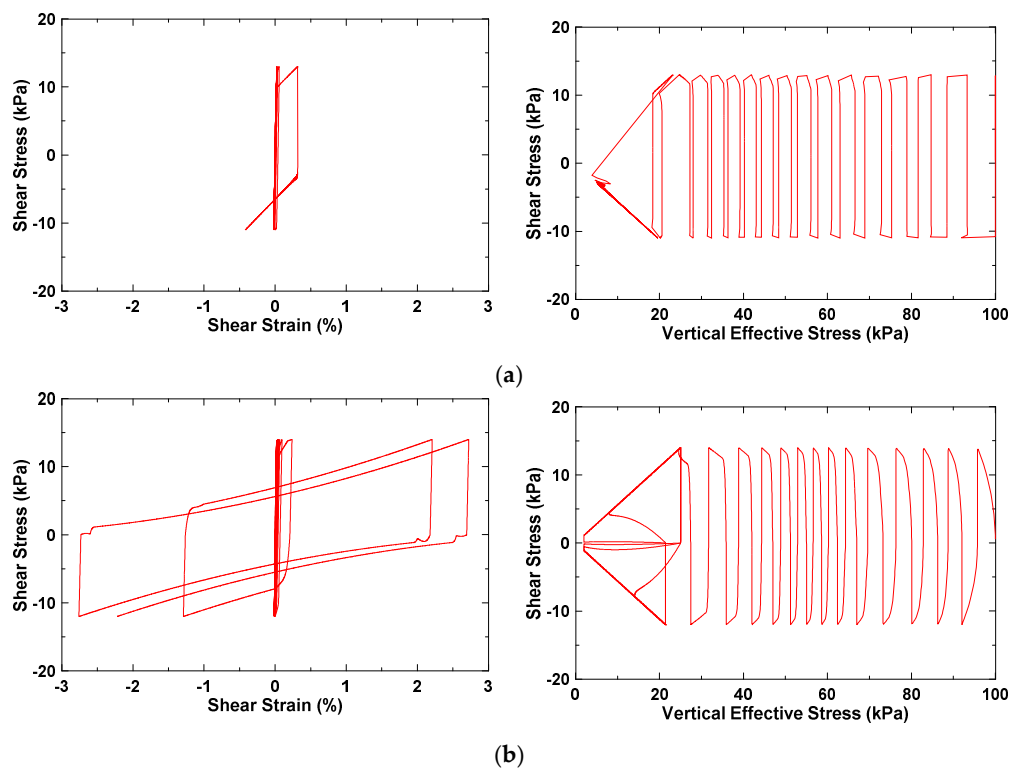


Figure 3. Undrained cyclic DSS loading response for $(N_1)_{60\text{cs}} = 10$ of the JRA96 procedure with vertical effective consolidation stress $\sigma_{vc}' = 101$ kPa and initial static shear stress = 0. (a) Finn model; (b) UBCSAND model.

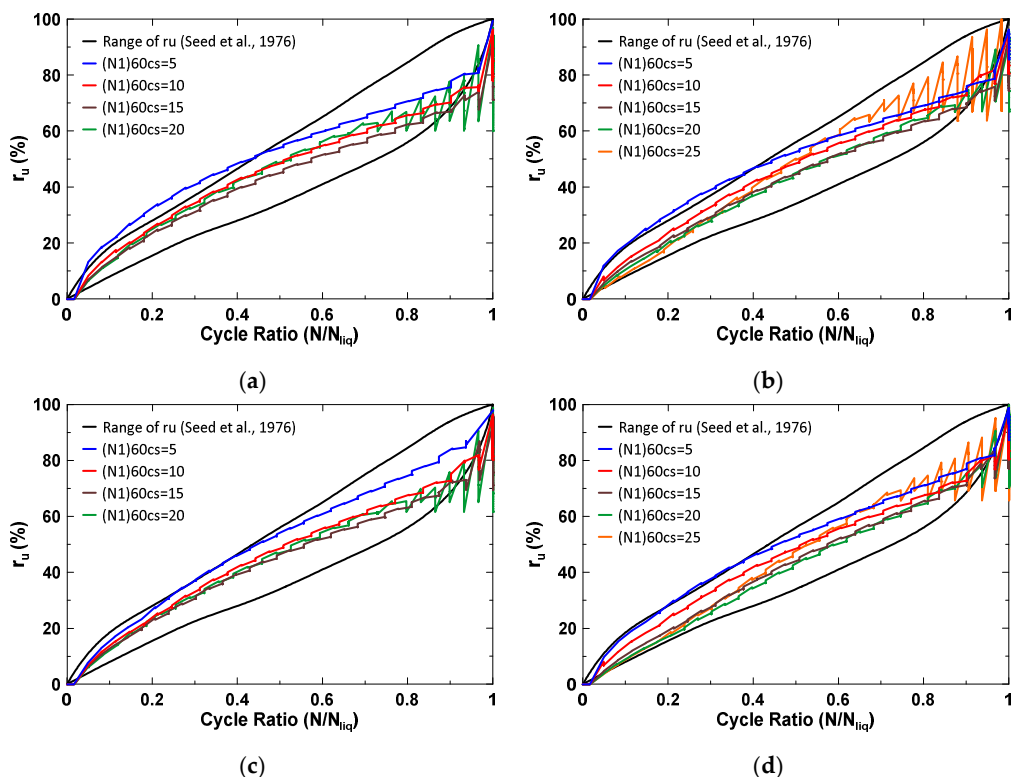


Figure 4. Accumulation of excess pore water pressure ratio and the associated cycle ratio of the Finn model. (a) HBF; (b) JRA96; (c) NCEER; (d) T-Y.

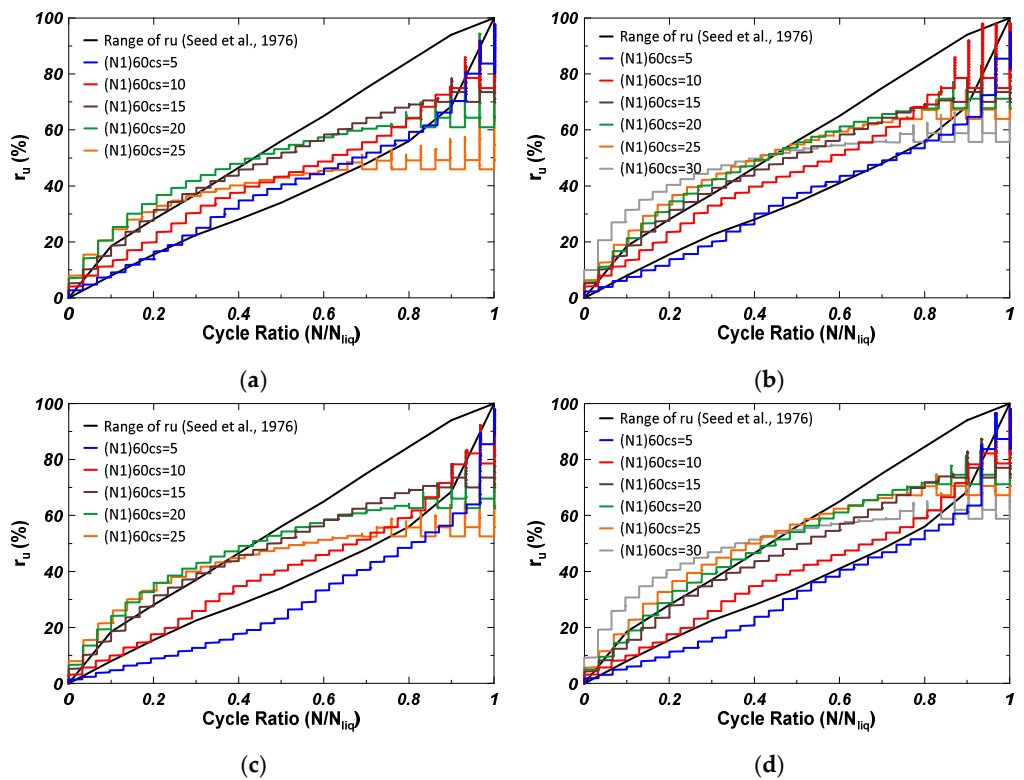


Figure 5. Accumulation of excess pore water pressure ratio and associated cycle ratio of the UBC-SAND model. (a) HBF; (b) JRA96; (c) NCEER; (d) T-Y.

Laboratory tests show that the CRR is related to the number of uniform loading cycles, N (related to the earthquake magnitude). The relationship between the CRR and N can be approximated with a power function:

$$\text{CRR} = a \times N^{-b}, \quad (14)$$

where a and b are determined by regression against the experimental data. The normalized CRR ($\text{CRR}/\text{CRR}_{N=15}$) versus N_{liq} curves (the weighting curves) are plotted in Figure 6 against the $b = 0.34$ (typical value for clean sand) curve [30]. The weighting curves of both models follow the trend of the typical clean sand curve, indicating that the effects of earthquake magnitude on the CRR could be adequately modeled.

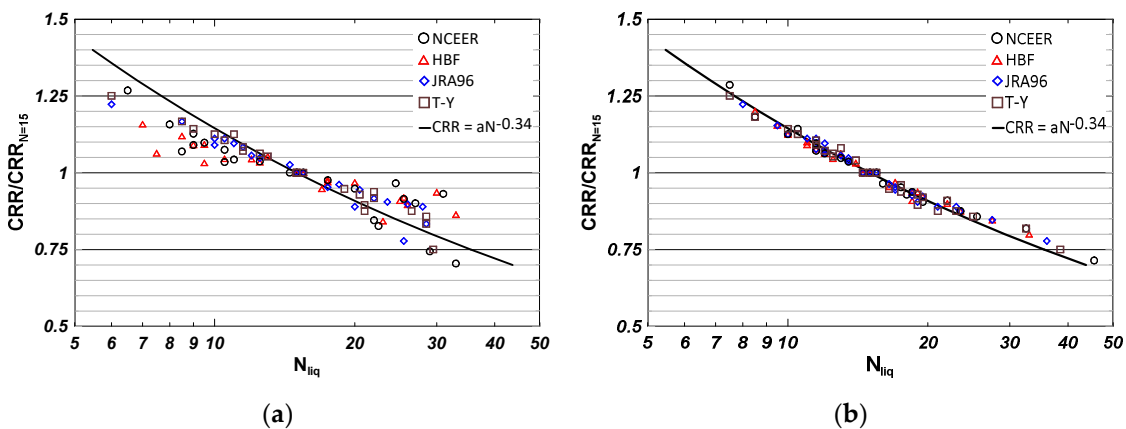


Figure 6. Weighting curves of four simplified liquefaction analysis procedures. (a) Finn model; (b) UBCSAND model.

The effects of the overburden stress and the static shear stress on the CRR were compared with published relationships for cases of the NCEER procedure (Figures 7 and 8) because only the NCEER procedure includes these effects in the CRR calculation. The overburden stress effect is represented by K_σ [30] and compared with the proposed relationships [10]:

$$K_\sigma = (\sigma_{vc}' / P_a)^{f-1}, \quad (15)$$

where σ_{vc}' is the vertical effective consolidation stress, P_a is the atmospheric pressure, and f is the model constant ($D_R = 40\text{--}60\%$ and $f = 0.8\text{--}0.7$, $D_R = 60\text{--}80\%$ and $f = 0.7\text{--}0.6$). The parameter m_hfac1 (refer to Tables 2 and 3) of the UBCSAND model is used to include the overburden stress effect. Using the calibrated relationships of m_hfac1 [19], Figure 7 shows that the K_σ of the UBCSAND model was in good agreement with the proposed curves [10]. The Finn model could capture the decrease in K_σ with increasing σ_{vc}' , but the effect of D_R on K_σ did not coincide well with those of the curves from the NCEER procedure.

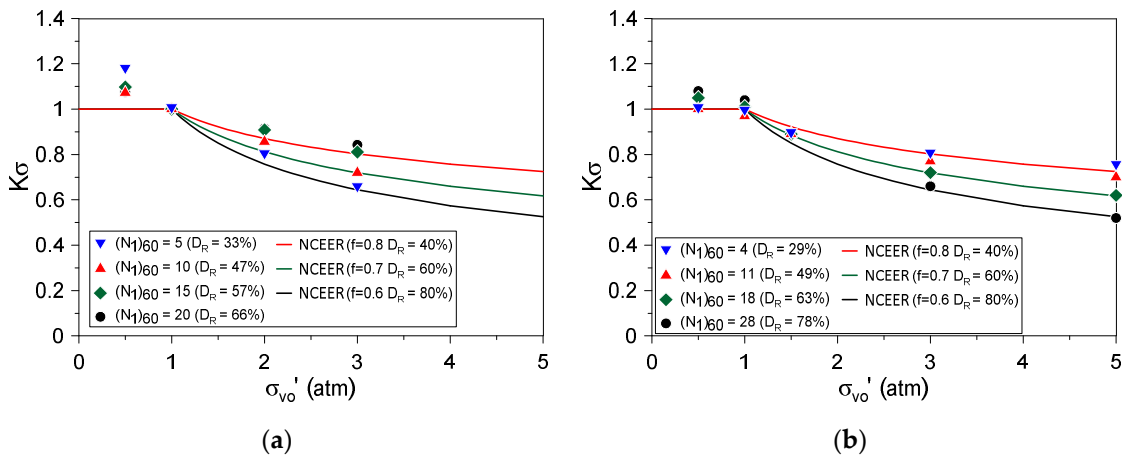


Figure 7. Overburden stress effects on the CRR and comparison with curves in the NCEER procedure. (a) Finn model; (b) UBCSAND model (modified from Beaty and Byrne, 2011) [19].

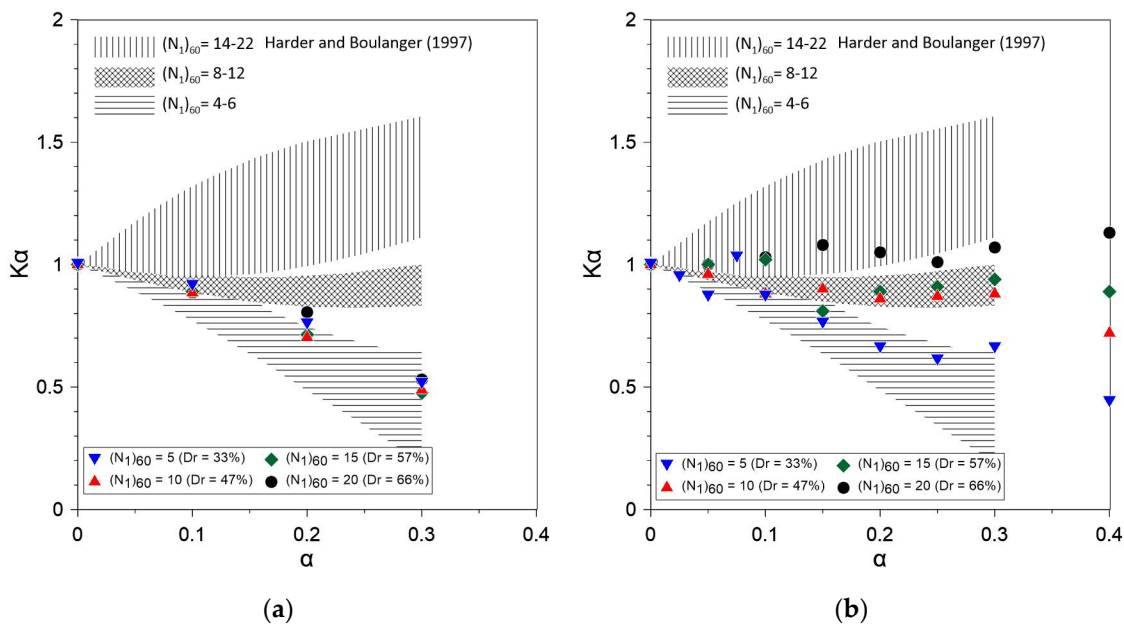


Figure 8. Static shear stress effects on the CRR and comparison with curves in the NCEER procedure. (a) Finn model; (b) model (modified from Beaty and Byrne, 2011) [19].

The effect of static shear stress on the CRR is represented by K_α [31] and compared with experimental data [32]. Figure 8 shows that the K_α of the UBCSAND model was in good agreement with experimental data. The Finn model captured the trend of K_α at the case of $(N_1)_{60} = 5$ only. In summary, K_σ and K_α were poorly modeled by the Finn model because the dilatant behavior of sand cannot be modeled appropriately by the simple formulation of the Finn model.

5. Conclusions

Soil-liquefaction-related hazards can damage structures via different mechanisms. In practice, the occurrence of soil liquefaction on a site is evaluated by a simplified liquefaction analysis procedure. Then, the damage of structures due to liquefaction hazards and the effectiveness of mitigation plans are explored by numerical simulation. Therefore, the liquefaction constitutive model used in numerical simulation should have a liquefaction resistance that is consistent with the simplified liquefaction analysis procedure in order to obtain reasonable and comparable evaluation results. In this study, the Finn model and the UBCSAND model were calibrated by fitting liquefaction triggering curves of four simplified liquefaction analysis procedures (NCEER, HBF, JRA96, and T-Y procedures). The calibration results are summarized as follows:

- (1) The Finn model was not capable of modeling the banana-shaped stress–strain path and the butterfly-shaped stress path observed in the laboratory test. In contrast, the UBCSAND model could approximately capture these behaviors by tracking the stress ratio history to modify the plastic shear modulus.
- (2) Both models provided reasonable simulations of the excess pore pressure accumulation during cyclic loadings.
- (3) The relationship between the CRR and the number of uniform loading cycles of the UBCSAND model fit the proposed curves [30] well. The Finn model simulation data deviated from the proposed curves but were still in a reasonable range. Thus, both models were able to adequately model the effects of earthquake magnitude on the CRR.
- (4) The UBCSAND model reasonably captured the overburden stress effect and the static shear stress effect on the CRR. Given that the dilatant behavior of sand is not included in the formulations of the Finn model, these effects on the CRR were poorly represented by the Finn model.
- (5) The Finn model can be used for the preliminary numerical simulation of structural damage caused by the strength reduction of the liquefiable soil. In general conditions, the UBCSAND model is highly recommended for numerical simulation to obtain reasonable and reliable results.
- (6) When the effect of liquefaction hazards or the effectiveness of a mitigation plan need to be evaluated via the numerical analysis, engineers can choose model input parameters according to the $(N_1)_{60\text{cs}}$ and the simplified liquefaction analysis procedure used in the evaluation of the soil liquefaction occurrence. Then, the numerical analysis can provide reasonable and comparable results.

Author Contributions: J.-C.C. developed the conceptualization; J.-C.C. and D.-G.L. worked on the methodology; J.-C.C. and H.-T.Y. performed the numerical analysis and analyzed the data; J.-C.C. prepared the draft manuscript; D.-G.L. revised the manuscript. All authors have read and agreed to the published version of the manuscript.

Funding: This research and the APC were funded by the Ministry of Science and Technology, Taiwan R.O.C. under Grant No. MOST 109-2221-E-005-007-MY3.

Institutional Review Board Statement: Not applicable.

Informed Consent Statement: Not applicable.

Data Availability Statement: Not applicable.

Acknowledgments: We would like to thank the Ministry of Science and Technology, Taiwan R.O.C., for its support under Grant No. MOST 109-2221-E-005-007-MY3. We also like to thank Der-Guey Lin for valuable suggestions on the numerical simulation.

Conflicts of Interest: The authors declare no conflict of interest.

References

1. Giannakou, A.; Travasarou, T.; Ugalde, J.; Chacko, J. Calibration Methodology for Liquefaction Problems Considering Level and Sloping Ground Conditions. In Proceedings of the 5th International Conference on Earthquake Geotechnical Engineering, Santiago, Chile, 11–13 January 2011. Paper No. CMFGI.
2. Beaty, M.H. Application of UBCSAND to the LEAP centrifuge experiments. *Soil Dyn. Earthq. Eng.* **2018**, *104*, 143–153. [CrossRef]
3. Anthi, M.; Gerolymos, N. A Calibration procedure for sand plasticity modeling in earthquake engineering: Application to TA-GER, UBCSAND and PM4SAND. In Proceedings of the 7th International Conference on Earthquake Geotechnical Engineering, Rome, Italy, 17–20 June 2019; pp. 17–20.
4. Giannakou, A.; Travasarou, T.; Chacko, J. Numerical Modeling of Liquefaction-Induced Slope Movements. In Proceedings of the GeoCongress 2012: State of the Art and Practice in Geotechnical Engineering, Oakland, CA, USA, 25–29 March 2012; pp. 663–672.
5. Shriro, M.; Bray, J.D. Calibration of Numerical Model for Liquefaction-Induced Effects on Levees and Embankments. In Proceedings of the 7th International Conference on Case Histories in Geotechnical Engineering, Chicago, IL, USA, 29 April–4 May 2013.
6. Choobbasti, A.J.; Selatahneh, H.; Petanlar, M.K. Effect of fines on liquefaction resistance of sand. *Innov. Infrastruct. Solut.* **2020**, *5*, 1–16. [CrossRef]
7. Soroush, A.; Koohi, S. Numerical analysis of liquefaction-induced lateral spreading. In Proceedings of the 13th World Conference on Earthquake Engineering, Vancouver, BC, Canada, 1–6 August 2004; p. 2123.
8. Iraji, A.; Osouli, A. Liquefaction Numerical Analysis of a Cantilevered Retaining Wall Using a Simple Finn-Byrne Model. In Proceedings of the Geo-Congress 2020: Geotechnical Earthquake Engineering and Special Topics, Minneapolis, MN, USA, 25–28 February 2020; pp. 41–50.
9. Elgamal, A.; Yang, Z.; Parra, E. Computational modeling of cyclic mobility and post-liquefaction site response. *Soil Dyn. Earthq. Eng.* **2002**, *22*, 259–271. [CrossRef]
10. Youd, T.L.; Idriss, I.M.; Andrus, R.D.; Arango, I.; Castro, G.; Christian, J.T.; Dobry, R.; Liam, F.W.D.; Harder, L.F., Jr.; Hynes, M.E.; et al. Liquefaction resistance of soils: Summary report from the 1996 NCEER and 1998 NCEER/NSF workshops on evaluation of liquefaction resistance of soils. *J. Geotech. Geoenviron. Eng. ASCE* **2011**, *127*, 817–833. [CrossRef]
11. Huang, J.H.; Chen, C.H.; Juang, C.H. Calibrating the model uncertainty of the HBF simplified method for assessing liquefaction potential of soils. *Sino-Geotech.* **2012**, *133*, 77–86. (In Chinese)
12. Japan Road Association (JRA). *Specification for Highway Bridges, Part. V: Seismic Design*; 1996, Substructures. Available online: <https://www.pwri.go.jp/eng/ujnr/joint/34/paper/53unjoh> (accessed on 4 June 2021).
13. Tokimatsu, K.; Yoshimi, Y. Empirical correlation of soil liquefaction based on SPT N-value and fines content. *Soils Found.* **1983**, *23*, 56–74. [CrossRef]
14. Martin, G.R.; Finn, W.L.; Seed, H.B. Fundamentals of liquefaction under cyclic loading. *J. Geotech. Geoenviron. Eng.* **1975**, *101*, 423–438.
15. Byrne, P.M. A Cyclic Shear-Volume Coupling and Pore-Pressure Model for Sand. In Proceedings of the Second International Conference on Recent Advances in Geotechnical Earthquake Engineering and Soil Dynamics, St. Louis, MO, USA, 11–15 March 1991; pp. 47–55.
16. Itasca. *FLAC: Fast Lagrangian Analysis of Continua*; Itasca Consulting Group Inc.: Minneapolis, MN, USA, 2011.
17. Puebla, H.; Byrne, P.M.; Phillips, R. Analysis of CANLEX liquefaction embankments: Prototype and centrifuge models. *Can. Geotech. J.* **1997**, *34*, 641–657. [CrossRef]
18. Beaty, M.; Byrne, P.M. An Effective Stress Model for Predicting Liquefaction Behaviour of Sand. *Geotech. Earthq. Eng. Soil Dyn. III ASCE* **1998**, *75*, 766–777.
19. Beaty, M.H.; Byrne, P.M. *UBCSAND Constitutive Model. Version 904aR*; Itasca UDM: Minneapolis, MN, USA, 2011; p. 69.
20. Yang, D.; Naesgaard, E.; Byrne, P.M.; Adalier, K.; Abdoun, T. Numerical model verification and calibration of George Massey Tunnel using centrifuge models. *Can. Geotech. J.* **2004**, *41*, 921–942. [CrossRef]
21. Chou, J.C. Centrifuge Modeling of the BART Transbay Tube and Numerical Simulation of Tunnels in Liquefying Ground. Ph.D. Dissertation, University of California, Los Angeles, CA, USA, 2010.
22. Bray, J.D.; Dashti, S. Liquefaction-induced building movements. *Bull. Earthq. Eng.* **2014**, *12*, 1129–1156. [CrossRef]
23. Ardeshiri-Lajimi, S.; Yazdani, M.; Assadi-Langroudi, A. A Study on the liquefaction risk in seismic design of foundations. *Geomech. Eng.* **2016**, *11*, 805–820. [CrossRef]
24. Chou, J.C.; Lin, D.G. Incorporating ground motion effects into Sasaki and Tamura prediction equations of liquefaction-induced uplift of underground structures. *Geomech. Eng.* **2020**, *22*, 25–33.
25. Seed, H.B.; Idriss, I.M. *Soil Moduli and Damping Factors for Dynamic Response Analysis*; University of California: Los Angeles, CA, USA, 1970; Rpt. No. UCB/EERC-70/10.

26. Seed, H.B.; Wong, R.T.; Idriss, I.M.; Tokimatsu, K. Moduli and damping factors for dynamic analyses of cohesionless soils. *J. Geotech. Eng.* **1986**, *112*, 1016–1032. [[CrossRef](#)]
27. Hardin, B.O.; Drnevich, V.P. Shear modulus and damping in soils: Measurement and parameter effects (Terzaghi Lecture). *J. Soil Mech. Found. Div.* **1972**, *98*, 603–624. [[CrossRef](#)]
28. Beaty, M.H.; Perlea, V.G. Several observations on advanced analyses with liquefiable materials. In Proceedings of the 31st Annual USSD Conference and 21st Conference on Century Dam Design-Advances and Adaptations, San Diego, CA, USA, 11–15 April 2011; pp. 1369–1397.
29. Seed, H.B.; Martin, P.P.; Lysmer, J. Pore-water pressure changes during soil liquefaction. *J. Geotech. Geoenviron. Eng.* **1976**, *102*, 323–346.
30. Idriss, I.M.; Boulanger, R.W. *Soil Liquefaction during Earthquakes*; Earthquake Engineering Research Institute: Oakland, CA, USA, 2008.
31. Seed, H.B. Earthquake Resistant Design of Earth Dams. In Proceedings of the Symposium on Seismic Design of Embankments and Caverns, Philadelphia, PA, USA, 6–10 May 1983; pp. 41–64.
32. Harder, L.F.; Boulanger, R.W. Application of $K\sigma$ and $K\alpha$ correction factors. In Proceedings of the NCEER Workshop on Evaluation of Liquefaction Resistance of Soils, Salt Lake City, Utah, USA, 5–6 January 1996; Youd, T.L., Idriss, I.M., Eds.; Technical Report NCEER-97-0022. National Center for Earthquake Engineering Research: Buffalo, NY, USA, 1997; pp. 167–190.